



# Journal of Applied and Computational Mechanics



Research Paper

## Behavior of Nanofluid with Variable Brownian and Thermal Diffusion Coefficients Adjacent to a Moving Vertical Plate

A.S. Rashed<sup>1,2</sup>, Tarek A. Mahmoud<sup>3</sup>, M.M. Kassem<sup>4</sup>

<sup>1</sup> Department of Physics and Engineering Mathematics, Faculty of Engineering, Zagazig University, Zagazig, 44515, Egypt, Email: ahmed.s.rashed@gmail.com

<sup>2</sup> Faculty of Engineering, Delta University for Science and Technology, Gamasa, Egypt

<sup>3</sup> Department of Physics and Engineering Mathematics, Faculty of Engineering, Zagazig University, Zagazig, 44515, Egypt, Email: tamibrahim@zu.edu.eg

<sup>4</sup> Department of Physics and Engineering Mathematics, Faculty of Engineering, Zagazig University, Zagazig, 44515, Egypt, Email: mkassem@live.com

Received August 21 2020; Revised December 07 2020; Accepted for publication January 25 2021.

Corresponding author: A.S. Rashed (ahmed.s.rashed@gmail.com)

© 2021 Published by Shahid Chamran University of Ahvaz

**Abstract.** This work was motivated by studying the behavior of nanofluid adjacent to a moving vertical plate. A non-homogeneous distribution of nanoparticles inside the boundary layer was considered with variable Brownian and thermal diffusion coefficients throughout the layer. Employing group similarity transformation method transformed the governing mathematical model into a system of ordinary differential equations. The resultant system was numerically solved using shooting method. The numerical investigation was carried out for different parameters namely: Prandtl number,  $Pr$ , temperature difference ratio,  $\gamma$ , and the ratio of nanoparticles volumetric fraction difference,  $\gamma_\phi$ , and the attained results were illustrated graphically to examine their effect on different fluid characteristics. The results showed that increasing  $Pr$  values decreased the nanofluid velocity, shear stress, temperature distribution and nanoparticles volumetric fraction, while it increased the heat flux and nanoparticles gradient inside the boundary layer. On the other hand, increasing  $\gamma$  values increased the nanofluid velocity, shear stress and heat flux but it decreased the temperature distribution. Also, increasing  $\gamma_\phi$  values decreased the nanofluid velocity, shear stress and temperature distribution but it increased the heat flux. The characteristics of nanofluids were studied to enhance the thermal conductivity and the efficiency of heat transfer systems. A comparison between the obtained results and the previous published results indicated an excellent agreement.

**Keywords:** Brownian diffusion coefficient; Group method; Nanofluids fluids; Prandtl number; Volumetric nanoparticles fraction.

### 1. Introduction

During the past few decades, the authors were being interested to the natural convective heat transfer from due to its importance in several applications such as heat transfer devices, cooling rate of vertical surfaces in an aquifer and heat losses from underground energy storage systems. The characteristics of the flow and heat transfer were investigated by analyses or experiments. The heat and mass transfer over the surface of a vertical plate in porous media represents the corner stone of several engineering and geophysical applications. The natural convection phenomenon occurs due to temperature difference, concentration difference, or combination of them. The applications include gas turbines, thermal energy storage, solar energy collectors, cooling of electronic equipment, cooling of nuclear reactors, heat transfer from a heater to room air, boilers, lubricants and space technology, petroleum industries, atmospheric and oceanic circulation.

New approaches of nanotechnology facilitated obtaining nanoparticles (typically 1-100 nm). One of the recent trends of nanotechnology applications is the formation of nanofluids. This type of fluid contains a base fluid incorporating suspended nanoparticles to modify different properties of the fluid like thermal and electrical conductivities. Researchers also have tried to create different types of nanoparticles using various methods like sol-gel process, chemical vapor deposition, plasma arcing and other numerous methods to fulfil the desired objective. Nanofluids have numerous engineering applications especially in heat transfer applications such as transformer cooling, fuel cells, engines with hybrid powers, engine cooling and solar water heating, microwave tubes, cooling and heating in buildings, heat exchangers, chillers and domestic refrigerators. This inspired some researchers to study the effect in case of nanofluids instead of traditional fluids [1, 2].

Two models are being used to describe the nanofluid dynamics, single-phase and two-phase models. In the heat transfer process, the two-phase model helps in understanding the functions of the fluid phase and the solid particles, so it is more convenient to model the nanofluid. In this work, two-phase model has been developed to avoid the limitations of single-phase model [3]. Both models have been exploited to describe many applications [4]. In single-phase model, the nanofluids are considered as common pure fluid and their only effect appears in thermal conductivity and viscosity. There is not any slip motion



between the nanoparticles and fluid molecules. So, the mixture of nanoparticles is uniform. In two-phase model, slip velocities are considered which play important role on the heat transfer performance of nanofluid [5]. So, the volume fraction of nanofluids is not uniform anymore and the concentration of nanoparticles in a mixture is variable.

Mathematical models of nanofluids consider many forces affecting the fluid like gravity, slip motion, friction, Brownian motion and other external forces. In non-homogeneous model, the convective transport models of nanofluid has been investigated [6]. A separate equation of concentration equation is solved by a two phase Buongiorno model [7]. Alumina ( $Al_2O_3$ ) has many important characteristics such as high melting point, high level of hardness, high stability, excellent heat and good electrical insulation. This allows alumina to be used in extreme conditions.  $Al_2O_3$  is one of the most important and widely used materials in structural applications because of its low cost and easy production process [8]. It has been exploited in cutting tool materials, energy and chemical fields [9, 10]. Alumina is also used in the surface protective coating, catalyst, insulator, and composite materials [11].

Khan and Aziz [12], Eastman [13] and Aziz [14] studied the convective heat transfer in nanofluids with different flow conditions for various geometries. Rahman [15] showed that the local rate of shear stress increases with an increase of the Brownian diffusion parameter (Nb) but it decreases with an increase of the magnetic field parameter, M. Siddiqua [16] concluded that the diffusivity ratio parameter (NA) and particle-density increment number (NB) have a significant impact on the reduction of heat transfer rate. Ibrahim [17] found that increasing Schmidt number and chemical reaction parameter results in a reduction of the velocity and concentration. Aly [18] stated that nanofluid velocity slip boundary condition is necessary and must be taken into consideration in nanoscale research. Elgazery [19] found that the distributions of velocity and temperature are affected by the types of nanofluids. Maskeen [20] found that the alumina nanoparticles achieve the highest velocity and the corresponding shear stress compared to other types of nanoparticles. Ferdows [21] showed that the maximum rate of heat transfer is obtained by adding alumina particles to the base fluid. Emad [22] concluded that the Nusselt number increases with increase of Prandtl number. Anuar [23] showed that ( $TiO_2$ -water) nanofluid has better Nusselt number compared to other nanofluids. Hojatollah [24] showed that increasing Prandtl number increases the Sherwood number.

Recently, several attempts have been developed to improve the thermal properties of nanofluid [25, 26]. Sheikholeslami [25] simulated the behavior of nanofluid under the impact of Lorentz force inside a porous curved cavity using Control Volume Finite Element. He concluded that decreasing magnetic forces decreases energy loss and stated that Bejan number is enhanced by improving conduction mode. The same author in [26] enhanced the rate of solidification in latent heat thermal energy storage systems (LHTES) by adding non-enhanced Common phase change material (NEPCM). He illustrated that solidification is obtained for diameter of nanoparticles ( $d_p = 40$  nm). Khan [27] investigated the heat transfer of mixed convective flow in a vertical plate using Laplace transform and found that the temperature decreases with increasing Prandtl number. Farhad [28] concluded that the velocity and temperature of the nanofluid decreases as the nanoparticle volume fraction increases. He found that ( $Al_2O_3 - H_2O$ ) nanofluid has the highest velocity compared to other nanofluids ( $TiO_2 - H_2O$ ,  $Cu - H_2O$  and  $Ag - H_2O$ ). Anwar [29] studied the free convection flow of some nanofluids over a vertical plate and concluded that the nanofluid velocity decreased by increasing the volume fraction  $\phi$  and magnetic parameter M. Also, the results profile showed that ( $Al_2O_3 - H_2O$ ) nanofluid admits the highest velocity compared to other nanofluids. Liancun [30] showed that increasing the fractal dimension ( $d_f$ ) leads to a reduction in both momentum and thermal boundary layers. Increasing the volume fraction of nanoparticles, a linear relation of the thermal layer and a nonlinear one of the momentum layer were obtained for different fractal dimensions. Khan [31] investigated the bioconvection in rotating disks by using Buongiorno's model and concluded that the temperature increases when Brownian and thermophoresis parameters increase. Ilyas Khan [32] studied the model related to the heat transfer rate of diathermic oils such as Engine-oil (EO) and Kerosene-oil (KO). He concluded that adding the nanoparticles would control the freezing point of the EO and KO at a very low temperature. El-Zahar [33] studied the convective flow of nanofluid comprising Alumina and Copper nanoparticles across a horizontal circular cylinder. The velocity has been degraded due to increasing nanoparticles volumetric fraction. Sobamowo [34] and Hamid [35] have reported results on heat transfer in nanofluids about the vertical plate. Nagendra [36], Narahari [37] and Sobamowo [34] showed that the velocity of the nanofluid and the temperature distribution in the boundary layer decrease as increase of the Prandtl number. Narahari [37] investigated the natural convection flow around a vertical plate with constant heat flux and concluded that the velocity, temperature and nanoparticle distribution are inversely related to Prandtl number. Das [38] showed that the fluid velocity and temperature increase with an increase of Grashof number. Rahman [39] concluded that the velocity of the nanofluid decreases as increase of the nanoparticle volume concentration. Sheikholeslami [40] showed that the concentration boundary layer thickness decreases with the increase of the Thermophoretic parameter. Ganji [41] investigated that the Nusselt number is directly proportional with the volume fraction of nanoparticles and the Eckert number. Ravnik [42] proved that the distribution of the temperature in the fluid and in the pipe is related to the concentration of the nanoparticle. Sandeep [43] indicated that the thermal Grashof number has a high effect on heat transfer rate in the case of the flow over a cone compared with the case of the edge or the plate. There is a good agreement between the obtained and the literature results.

Different techniques of similarity transformations have been widely employed to investigate either evolution equations in different dimensions or fluid dynamics described by Navier-Stokes equations [44-51]. The specific form for the invariants is defined by the solution of this set [52]. Abd El Malek [53] used such technique in order to provide effective analysis of varied boundary layer flow problems [46, 52, 54]. The convection flow of two-phase dusty nanofluid is modeled along a vertical plate. In this study, the governing systems of partial differential equations (PDEs) are transformed a coupled system of non-linear ordinary differential equations (ODEs) using the group and similarity transformations. The effect of Prandtl number (Pr), the ratio of wall and fluid temperature difference to absolute temperature  $\gamma$  and the ratio of nanoparticles volumetric fraction  $\gamma_\phi$  on the velocity, shear stress, temperature, heat flux and concentration are illustrated graphically and discussed in detail. Brownian motion is defined as the random motion of nanoparticles within the base fluid. The Brownian motion arises due to the collisions between the nanoparticles and the molecules of the base fluid. Brownian motion is given by the Einstein-Stokes's equation. Here  $K_B$  is the Boltzmann's constant and  $T$  is the nanofluid temperature [55]. In the present study, the Brownian diffusion coefficient  $D_b = (K_B / 3\pi\mu d_p)T$  is considered as function of nanofluid temperature  $T$ . These assumptions imply that change in temperature results in changing Brownian motion. Where the temperature is a function of variables  $x$  and  $y$ . Many researchers [19, 34, 38, 56] studied the properties of nanofluid flow around a vertical plate without concentration equation in their model. In our model, four equations (two mass equation, momentum equation and energy equation) have been used to fully describe and predict the behavior of nanofluid. In the present work the Brownian ( $D_b$ ) and thermal diffusion coefficients ( $D_T$ ) are functions of temperature ( $T$ ) and volume fraction ( $\phi$ ) which in turn are functions in the spatial variables,  $x$  and  $y$ . This is nearly not considered previously in the literature. This led to more complicated mathematical model which was accompanied by arbitrary boundary conditions to be discover during the analysis.



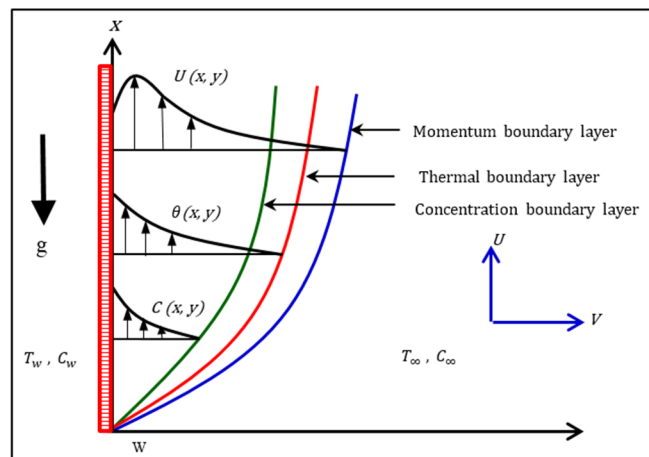


Fig. 1. Geometrical representation of the problem

## 2. Mathematical formulation

The present study considers a mathematical analysis for the case of a moving vertical plate through non-homogenous nanofluid. The analysis assumes laminar boundary layer is two-dimensional, Newtonian and steady state fluid dynamics. The flow configurations and the geometry of the problem are shown in Fig. (1). The governing boundary layer equations for two-dimensional flow can be written as :[55, 57].

$$\nabla \cdot \mathbf{V} = 0 \quad (1)$$

$$\mathbf{V} \cdot \nabla \phi = \nabla \cdot \left[ D_B \nabla \phi + D_T \frac{\nabla T}{T} \right] \quad (2)$$

$$[\mathbf{V} \cdot \nabla T] = \nabla \cdot \left[ \frac{k_{bf}}{\rho c_{bf}} \nabla T + \left( \frac{\rho c_{np}}{\rho c_{bf}} \right) \left[ D_B \nabla \phi \cdot \nabla T + D_T \frac{\nabla T \cdot \nabla T}{T} \right] \right] \quad (3)$$

$$u \frac{\partial u}{\partial x} + v \frac{\partial u}{\partial y} = \nu \frac{\partial^2 u}{\partial y^2} + g\beta(T - T_\infty) \quad (4)$$

Subjected to the following boundary conditions:

$$u(x,0) = u_w(x), \quad v(x,0) = 0, \quad \phi(x,0) = \phi_w, \quad T(x,0) = T_w \quad (5)$$

$$u(x,\infty) = 0, \quad v(x,\infty) = 0, \quad \phi(x,\infty) = \phi_\infty, \quad T(x,\infty) = T_\infty \quad (6)$$

where  $D_B = K_B T / (3\pi\mu d_p)$  and  $D_T = 0.26K_{bf}\mu\phi / (2K_{bf} + k_{np})\rho$ .

The physical quantities  $\rho_{bf}$ ,  $(C_p)_{bf}$  and  $k_{bf}$  are the density, specific heat and thermal conductivity of the base fluid while  $\rho_{np}$ ,  $(C_p)_{np}$  and  $k_{np}$  respectively are the same for the solid nanoparticle as illustrated in Table 1.

The following transformations are used to normalize the boundary conditions:

$$u(x,y) = u_w(x)U(x,y), \quad \theta = \frac{T - T_\infty}{T_w - T_\infty}, \quad C = \frac{\phi - \phi_\infty}{\phi_w - \phi_\infty} \quad (7)$$

Using (7), the governing equations and the corresponding boundary conditions, (1) - (6), are transformed to:

$$u_w \frac{\partial u}{\partial x} + U \frac{du_w}{dx} + \frac{\partial v}{\partial y} = 0 \quad (8)$$

$$(\Delta\phi)u_w U \frac{\partial C}{\partial x} + (\Delta\phi)v \frac{\partial C}{\partial y} = \delta \left[ (\Delta\phi)(\Delta T)\theta_y C_y + ((\Delta T)\theta + T_\infty)(\Delta\phi)C_{yy} \right] + \beta^* \left[ \left( \frac{(\Delta\phi)C + \phi_\infty}{((\Delta T)\theta + T_\infty)^2} \right) (\Delta T)\theta_{yy} + \left( \frac{(\Delta\phi)(\Delta T)}{((\Delta T)\theta + T_\infty)} \right) C_y \theta_y - \left( \frac{(\Delta\phi)C + \phi_\infty}{((\Delta T)\theta + T_\infty)} \right) (\Delta T)^2 \theta_y^2 \right] \quad (9)$$

$$(\Delta T)u_w U \theta_x + (\Delta T)v \theta_y = \alpha(\Delta T)\theta_{yy} + \left( \frac{\rho c_{np}}{\rho c_{bf}} \right) \left[ \delta(\Delta\phi)(\Delta T)\theta_y C_y ((\Delta T)\theta + T_\infty) + \beta^* (\Delta T)^2 \left( \frac{(\Delta\phi)C + \phi_\infty}{((\Delta T)\theta + T_\infty)} \right) \theta_y^2 \right] \quad (10)$$

$$u_w \frac{du_w}{dx} U^2 + u_w^2 U \frac{\partial U}{\partial x} + u_w v \frac{\partial U}{\partial y} = \nu u_w \frac{\partial^2 U}{\partial y^2} + g\beta(\Delta T)\theta \quad (11)$$



**Table 1.** Physical properties of the base fluid and nanoparticles [58, 59]

Physical properties	Fluid Phase (H <sub>2</sub> O)	Alumina (Al <sub>2</sub> O <sub>3</sub> )	Copper (Cu)	Titanium oxide (TiO <sub>2</sub> )	Silver (Ag)
C <sub>p</sub> (J / kgK)	4179	765	385	686.2	235
ρ (kg / m <sup>3</sup> )	997.1	3970	8933	4250	10500
k (w / mK)	0.613	40	400	8.9538	429

subjected to:

$$U(x, 0) = 1, v(x, 0) = 0, C(x, 0) = 1, \theta(x, 0) = 1 \quad (12)$$

$$U(x, \infty) = 0, v(x, \infty) = 0, C(x, \infty) = 0, \theta(x, \infty) = 0 \quad (13)$$

where  $\delta = K_b / 3\pi\mu d_p$  and  $\beta^* = 0.26K_{bf}\mu / (2K_{bf} + K_{np})\rho$ ,  $\Delta T = T_w - T_\infty$  and  $\Delta\phi = \phi_w - \phi_\infty$

### 3. Group formulation of the problem

The system of ordinary differential equations is being obtained from the equations (8) – (11) throughout one parameter group  $G$  defined as follows:

$$G: \bar{S} = Q^s(a)S + T^s(a) \quad (14)$$

where  $S$  and  $\bar{S}$  represent the variables of the system before and after the transformation,  $Q^s$  and  $T^s$  are real-valued coefficients and differentiable with respect to the group parameter ( $a$ ). Partial derivatives for the dependent variables with respect to independent variables are expressed as:

$$\left. \begin{aligned} \bar{S}_i &= \left( \frac{Q^s}{Q^i} \right) S_i \\ \bar{S}_{i,j} &= \left( \frac{Q^s}{Q^i Q^j} \right) S_{ij} \end{aligned} \right\} i, j = x, y \quad (15)$$

where  $S$  represents the dependent Variables ( $U, u_w, V, \theta$  and  $C$ ). A transformation of (8) - (11) following (14) and (15) definitions lead to:

$$\bar{u}_w \frac{\partial \bar{u}}{\partial \bar{x}} + \bar{u} \frac{d\bar{u}_w}{d\bar{x}} + \frac{\partial \bar{v}}{\partial \bar{y}} = H_1(a) \left[ u_w \frac{\partial u}{\partial x} + u \frac{du_w}{dx} + \frac{\partial v}{\partial y} \right] \quad (16)$$

$$\begin{aligned} & (\Delta\phi) \bar{u}_w \bar{U} \frac{\partial \bar{C}}{\partial \bar{x}} + (\Delta\phi) \bar{v} \frac{\partial \bar{C}}{\partial \bar{y}} - \delta \left[ (\Delta\phi)(\Delta T) \frac{\partial \bar{\theta}}{\partial \bar{y}} \frac{\partial \bar{C}}{\partial \bar{y}} + ((\Delta T)\bar{\theta} + T_\infty)(\Delta\phi) \frac{\partial^2 \bar{C}}{\partial^2 \bar{y}} \right] \\ & - \beta^* \left[ \left( \frac{(\Delta\phi)\bar{C} + \phi_\infty}{((\Delta T)\bar{\theta} + T_\infty)^2} \right) (\Delta T) \frac{\partial^2 \bar{\theta}}{\partial^2 \bar{y}} + \left( \frac{(\Delta\phi)(\Delta T)}{(\Delta T)\bar{\theta} + T_\infty} \right) \frac{\partial \bar{C}}{\partial \bar{y}} \frac{\partial \bar{\theta}}{\partial \bar{y}} - \left( \frac{(\Delta\phi)\bar{C} + \phi_\infty}{(\Delta T)\bar{\theta} + T_\infty} \right) (\Delta T)^2 \left( \frac{\partial \bar{\theta}}{\partial \bar{y}} \right)^2 \right] = \\ & H_2(a) \left[ \left( \Delta\phi \right) u_w U \frac{\partial C}{\partial x} + (\Delta\phi) v \frac{\partial C}{\partial y} - \delta \left[ (\Delta\phi)(\Delta T) \frac{\partial \theta}{\partial y} \frac{\partial C}{\partial y} + ((\Delta T)\theta + T_\infty)(\Delta\phi) \frac{\partial^2 C}{\partial^2 y} \right] \right. \\ & \left. - \beta^* \left[ \left( \frac{(\Delta\phi)C + \phi_\infty}{((\Delta T)\theta + T_\infty)^2} \right) (\Delta T) \frac{\partial^2 \theta}{\partial^2 y} + \left( \frac{(\Delta\phi)(\Delta T)}{(\Delta T)\theta + T_\infty} \right) \frac{\partial C}{\partial y} \frac{\partial \theta}{\partial y} - \left( \frac{(\Delta\phi)C + \phi_\infty}{(\Delta T)\theta + T_\infty} \right) (\Delta T)^2 \left( \frac{\partial \theta}{\partial y} \right)^2 \right] \right] \end{aligned} \quad (17)$$

$$H_3(a) \left[ (\Delta T) u_w U \frac{\partial \theta}{\partial x} + (\Delta T) v \frac{\partial \theta}{\partial y} - \alpha (\Delta T) \frac{\partial^2 \theta}{\partial^2 y} - \left( \frac{\rho C_{np}}{\rho C_{bf}} \right) \left[ \delta (\Delta\phi)(\Delta T) \frac{\partial \theta}{\partial y} \frac{\partial C}{\partial y} + ((\Delta T)\theta + T_\infty) + \beta^* (\Delta T)^2 \left( \frac{(\Delta\phi)C + \phi_\infty}{(\Delta T)\theta + T_\infty} \right) \left( \frac{\partial \theta}{\partial y} \right)^2 \right] \right] \quad (18)$$

$$\bar{u}_w \frac{d\bar{u}_w}{d\bar{x}} \bar{U}^2 + \bar{u}_w^2 \bar{U} \frac{\partial \bar{u}}{\partial \bar{x}} + \bar{u}_w \bar{v} \frac{\partial \bar{u}}{\partial \bar{y}} - v \bar{u}_w \frac{\partial^2 \bar{u}}{\partial^2 \bar{y}} - g\beta(\Delta T)\bar{\theta} = H_4(a) \left[ u_w \frac{du_w}{dx} U^2 + u_w^2 U \frac{\partial U}{\partial x} + u_w v \frac{\partial U}{\partial y} - v u_w \frac{\partial^2 U}{\partial y^2} - g\beta(\Delta T)\theta \right] \quad (19)$$

For invariant transformation of (16) - (19) and invariance of boundary conditions (12), the following results have been obtained:

$$T^U = T^{u_w} = T^v = T^\theta = T^C = T^y = 0 \quad (20)$$

$$\frac{Q^{u_w} Q^U}{Q^x} = \frac{Q^v}{Q^y} = H_1(a) \quad (21)$$

$$\frac{Q^{u_w} Q^U Q^C}{Q^x} = \frac{Q^v Q^C}{Q^y} = \frac{Q^C Q^\theta}{(Q^y)^2} = \frac{Q^C}{(Q^y)^2} = H_2(a) \quad (22)$$



$$\frac{Q^{U_w} Q^U Q^\theta}{Q^x} = \frac{Q^v Q^\theta}{Q^y} = \frac{Q^\theta}{(Q^y)^2} = \frac{Q^C (Q^\theta)^2}{(Q^y)^2} = \frac{Q^C Q^\theta}{(Q^y)^2} = H_3(a) \quad (23)$$

$$\frac{(Q^{U_w} Q^U)^2}{Q^x} = \frac{Q^{U_w} Q^U Q^v}{Q^y} = \frac{Q^{U_w} Q^U}{(Q^y)^2} = Q^\theta = H_4(a) \quad (24)$$

Combining equations (20) - (24) leads to:

$$Q^\theta = Q^C = 1, \quad Q^x = (Q^y)^4 \quad (25)$$

$$Q^v = \frac{1}{Q^y}, \quad Q^U = \frac{(Q^y)^2}{Q^{U_w}} \quad (26)$$

Now, the following group structure is being obtained:

$$G = \left\{ \begin{array}{l} G_1 \left\{ \begin{array}{l} \bar{x} = (Q^y)^4 x + T^x \\ \bar{y} = Q^y y \end{array} \right. \\ \bar{U} = \frac{(Q^y)^2}{Q^{U_w}} U \\ \bar{U}_w = Q^{U_w} U_w \\ G_2 \left\{ \begin{array}{l} \bar{C} = C \\ \bar{\theta} = \theta \\ \bar{V} = \frac{1}{Q^y} V \end{array} \right. \end{array} \right. \quad (27)$$

where  $G_1$  and  $G_2$  are the independent and dependent variables, respectively.

### 3.1. Group transformation of the system

In order to reduce the governing equations into a simpler form of ODEs system, Morgan theorem is applied [60] as follows:

$$\sum_{i=1}^7 (\alpha_i s_i + \beta_i) \frac{\partial \bar{s}_i}{\partial s_i} = 0 \quad (28)$$

where  $s_i$  and  $\bar{s}_i$  are the variables before and after transformation, respectively. Moreover, the coefficients  $\alpha_i$  and  $\beta_i$  are defined as:

$$\alpha_i = \frac{\partial Q^{s_i}(a)}{\partial a}, \quad \beta_i = \frac{\partial T^{s_i}(a)}{\partial a} \quad (29)$$

### 3.2. Transformation of the independent variables

Invoking (28), the similarity variable,  $\eta(x, y)$ , is obtained through:

$$(\alpha_1 x + \beta_1) \frac{\partial \eta}{\partial x} + \alpha_2 y \frac{\partial \eta}{\partial y} = 0 \quad (30)$$

The general solution of this equation is:

$$\eta(x, y) = y\pi(x) \quad (31)$$

where the function  $\pi(x)$  is to be determined later.

### 3.3 Transformation of the dependent variables

The invariant transformations of the dependent variables  $\bar{C}$ ,  $\bar{\theta}$ ,  $\bar{u}_w$ ,  $\bar{u}$  and  $\bar{v}$  inside the boundary layer are obtained by the group structure (3.14) and Morgan theorem described in (28):

$$\bar{C}(\bar{x}, \bar{y}) = C(\eta) \quad (32)$$

$$\bar{\theta}(\bar{x}, \bar{y}) = \theta(\eta) \quad (33)$$

$$\bar{u}_w(\bar{x}) = u_w(x) \quad (34)$$

$$\bar{u}(\bar{x}, \bar{y}) = w(x)F(\eta) \quad (35)$$

$$\bar{v}(\bar{x}, \bar{y}) = \Gamma(x)E(\eta) \quad (36)$$



### 3.4. Reduction of the problem to a system of ordinary differential equations

Equations (8) - (11) will be transformed throughout similarity variables described earlier. The result is illustrated hereafter: Equation (8) is transformed to:

$$\frac{dE}{d\eta} + (A_1 + A_2)F + A_3\eta \frac{dF}{d\eta} = 0 \quad (37)$$

where

$$A_1 = \frac{u_w}{\Gamma\pi} \frac{dw}{dx}, A_2 = \frac{w}{\Gamma\pi} \frac{du_w}{dx}, A_3 = \frac{u_w w}{\Gamma\pi^2} \frac{d\pi}{dx} \quad (38)$$

Similarly, (11) is reduced to:

$$\frac{\partial^2 F}{\partial \eta^2} + \left( \frac{g\beta\Delta T}{v} \right) A_4 \theta - (A_5 + A_6)F^2 - A_7\eta FF' - A_8EF' = 0 \quad (39)$$

where

$$A_4 = \frac{1}{(u_w\pi^2 w)}, A_5 = \frac{w}{v\pi^2} \frac{du_w}{dx}, A_6 = \frac{u_w}{v\pi^2} \frac{dw}{dx}, A_7 = \frac{u_w w}{v\pi^3} \frac{d\pi}{dx}, A_8 = \frac{\Gamma}{v\pi} \quad (40)$$

To this moment, the Eqs. (37) and (39) are considered ODEs if the relations described by (38) and (39) are constants. So, one can get:

$$\Gamma(x) = \sqrt{v} x^{\frac{-1}{4}}, \pi(x) = \frac{1}{\sqrt{v} x^{\frac{1}{4}}}, w(x) = bx^c, u_w(x) = \frac{1}{b} x^{\frac{1}{4}-c}, \eta(x, y) = \frac{y}{\sqrt{v} x^{\frac{1}{4}}} \quad (41)$$

and

$$A_1 = A_6 = c, A_2 = A_5 = \frac{1}{2} - c, A_3 = A_7 = -\frac{1}{4}, A_4 = v, A_8 = 1 \quad (42)$$

Using these results, Eqs. (9) and (10) are reduced to:

$$C'' = \frac{1}{(\Delta T \theta + T_\infty)} \left[ -\frac{v}{4\delta} \eta FC' + \frac{v}{\delta} EC' - \Delta T \theta' C' + \frac{B^* (\Delta T)^2}{\delta (\Delta \phi)} \left( \frac{\Delta \phi C + \phi_\infty}{(\Delta T \theta + T_\infty)^2} \right) (\theta')^2 - \frac{B^* (\Delta T)}{\delta (\Delta \phi)} \left( \frac{\Delta \phi C + \phi_\infty}{\Delta T \theta + T_\infty} \right) \theta'' - \frac{B^* (\Delta T)}{\delta} \left( \frac{C'}{\Delta T \theta + T_\infty} \right) \right] \quad (43)$$

$$\theta'' = \frac{-Pr}{4} \eta F \theta' + Pr E \theta' - \left( \frac{\rho C_{np}}{\rho C_{bf}} \right) \left[ \frac{\delta (\Delta \phi)}{\alpha} ((\Delta T) \theta + T_\infty) \theta' C' + \frac{\beta^* (\Delta T)}{\alpha} \left( \frac{\Delta \phi C + \phi_\infty}{\Delta \phi \theta + T_\infty} \right) (\theta')^2 \right] \quad (44)$$

Subjected to the boundary conditions:

$$\eta = 0 \begin{cases} E(0) = 0 \\ F(0) = 1 \\ \theta(0) = 1 \\ C(0) = 1 \end{cases} \quad \eta = \infty \begin{cases} F(\infty) = 0 \\ \theta(\infty) = 0 \\ C(\infty) = 0 \end{cases} \quad (45)$$

The interested physical quantities in our work are the local Nusselt number and Sherwood number [61]. The average Nusselt number is used to express the rate of heat transfer coefficient at the plate which is given by:

$$Nu = - \left( \frac{\partial \theta}{\partial \eta} \right)_{\eta=0} \quad (46)$$

The reduced Sherwood number as important parameter in mass transfer, can be obtained as:

$$Sh = - \left( \frac{\partial \phi}{\partial \eta} \right)_{\eta=0} \quad (47)$$

## 4. Numerical results and discussion

The behaviors of nanofluid over a moving vertical plate are investigated. The resulting system of ODEs (37) - (44) with the corresponding boundary conditions (45) is solved numerically by using MATLAB. The solution is adjusted at error tolerance of  $10^{-6}$ . For nanofluid, water is considered as base fluid and Alumina ( $Al_2O_3$ ) is used as nanoparticles. The effect of Prandtl number, Pr, the ratio of wall and fluid temperature difference to absolute temperature,  $\gamma$ , and the ratio of nanoparticles volumetric fraction,  $\gamma_\phi$ , are considered to be the study parameters. The numerical values of the Nusselt number and Sherwood number are computed as illustrated in tables 3, 4, 5 and 6. In the present study the following default parameter values are adopted for computations:  $d_p = 40nm$ ,  $\phi_w = 0.01$ ,  $T_\infty = 300K$ ,  $g\beta = 1$ .



#### 4.1 Effect of Prandtl number, Pr

The change in the Prandtl number inside the boundary and its effect on the nanofluid characteristics was considered. This is physically interpreted by changing the viscosity of the fluid. Computations were performed for the following range of Prandtl number ( $Pr$ ) parameter ( $2 \leq Pr \leq 5$ ). The numerical results showed that increasing  $Pr$  values led to a decrease in velocity amplitude due to the increment in the fluid viscosity as illustrated in Fig.2. This is followed by a corresponding decrement in shear stress due to the friction between nanofluid layers as shown in Fig.3. Moreover, the increase in  $Pr$  values results in a reduction in temperature distribution along the boundary layer thickness as shown in Fig.4. The maximum value of the fluid temperature is found near the surface of the plate and the temperature decays far away from the plate surface. Furthermore, increasing the Prandtl number increases the heat flux as shown in Fig.5. Obviously, Figs. 6 and 7 illustrate a decrease in nanoparticles volumetric fraction and an increase in nanoparticles gradient, respectively throughout the boundary layer because the high viscosity obstruct the movement of the nanoparticles.

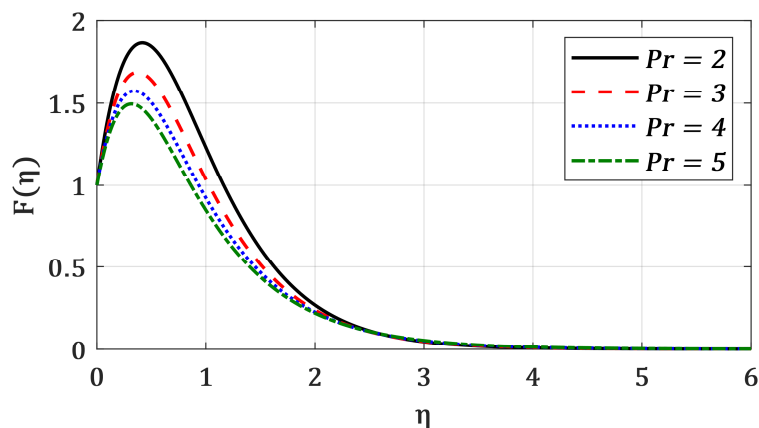


Fig. 2. Effect of Prandtl number on velocity of nanofluid inside the boundary layer when  $\gamma = 0.05, \gamma_\varphi = 2$  ( $\text{Al}_2\text{O}_3$ -water)

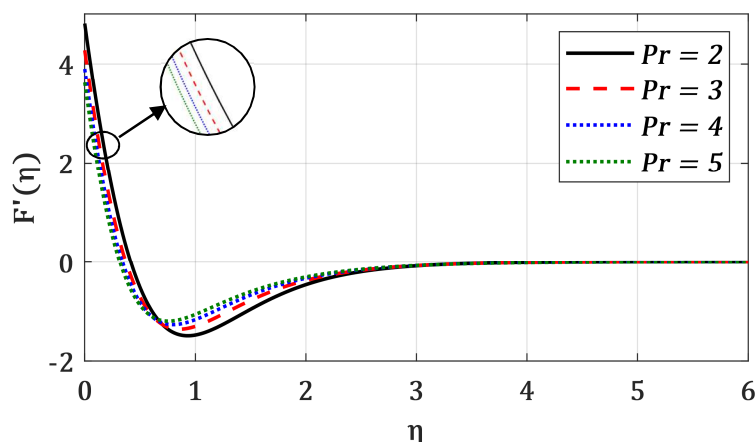


Fig. 3. Effect of Prandtl number on shear stress of nanofluid inside the boundary layer when  $\gamma = 0.05, \gamma_\varphi = 2$  ( $\text{Al}_2\text{O}_3$ -water)

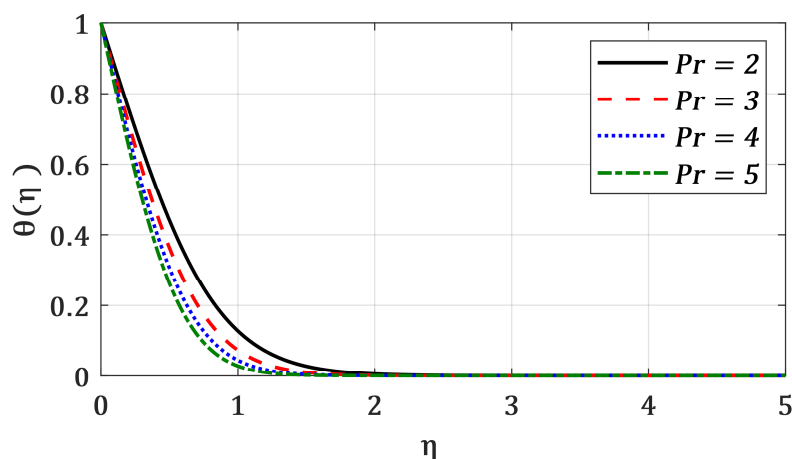


Fig. 4. Effect of Prandtl number on temperature distribution of nanofluid inside the boundary layer when  $\gamma = 0.05, \gamma_\varphi = 2$  ( $\text{Al}_2\text{O}_3$ -water)





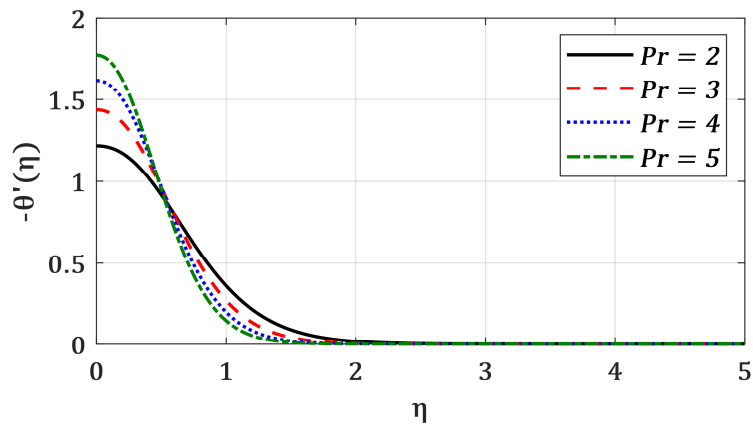


Fig. 5. Effect of Prandtl number on heat flux of nanofluid inside the boundary layer w when  $\gamma = 0.05, \gamma_\varphi = 2$  ( $\text{Al}_2\text{O}_3$ -water)

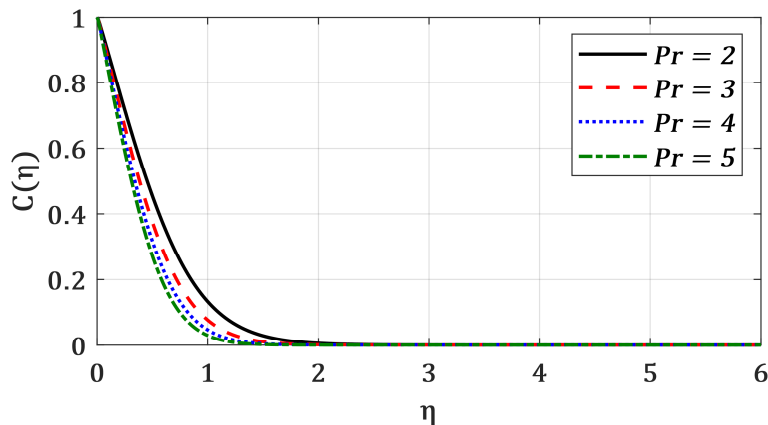


Fig. 6. Effect of Prandtl number on nanoparticles volumetric fraction distribution of nanofluid inside the boundary layer when  $\gamma = 0.05, \gamma_\varphi = 2$  ( $\text{Al}_2\text{O}_3$ -water)

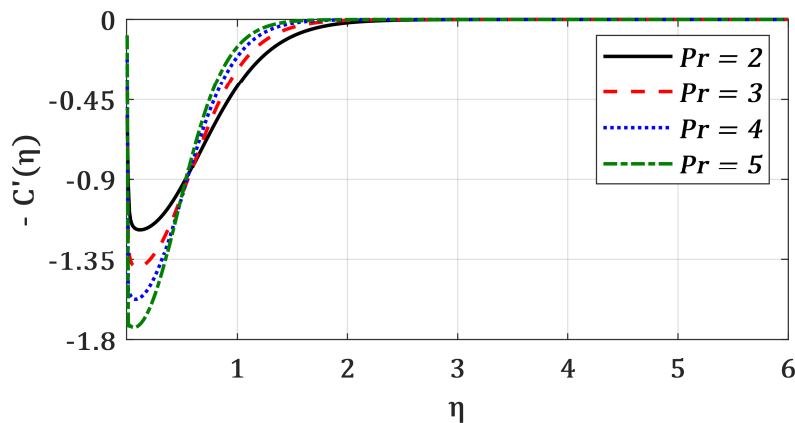


Fig. 7. Effect of Prandtl number on gradient of nanoparticles volumetric fraction of nanofluid inside the boundary layer when  $\gamma = 0.05, \gamma_\varphi = 2$  ( $\text{Al}_2\text{O}_3$ -water)

For validation of the numerical method used in this study, the present results are compared to the results reported by researchers [35]. Table 2 shows the quantitative comparison, which is found to be in a very good agreement. In the case of the effect of the Prandtl number,  $Pr$ , on the temperature, a comparison between the present study and the result reported by Hamid [35] is presented. From Tables 2 and Fig. 8, it can be noted that there is an excellent agreement with these approaches and thus the accuracy of the method is verified.

Table 2. Numerical results of the temperature  $\theta(\eta)$  for various values of  $Pr$  with  $\gamma = 0.02, \gamma_\varphi = 2, T_\infty = 300 \text{ K}, \varphi_\infty = 0.01$ .

		$\theta(\eta)$					
		$\eta = 0$	$\eta = 1$	$\eta = 2$	$\eta = 3$	$\eta = 4$	$\eta = 5$
$Pr = 1$	Hamid[35]	1	0.39016	0.102831	0.02254	0.00396	0
	Present Results	1	0.36577	0.086261	0.01676	0.00307	0
$Pr = 2$	Hamid[35]	1	0.198314	0.019832	0.000282	0	0
	Present Results	1	0.129666	0.005249	1.5312e-04	0	0
$Pr = 3$	Hamid[35]	1	0.1105165	0.003251	0.000049	0	0
	Present Results	1	0.10501	0.00282	0.000046	0	0





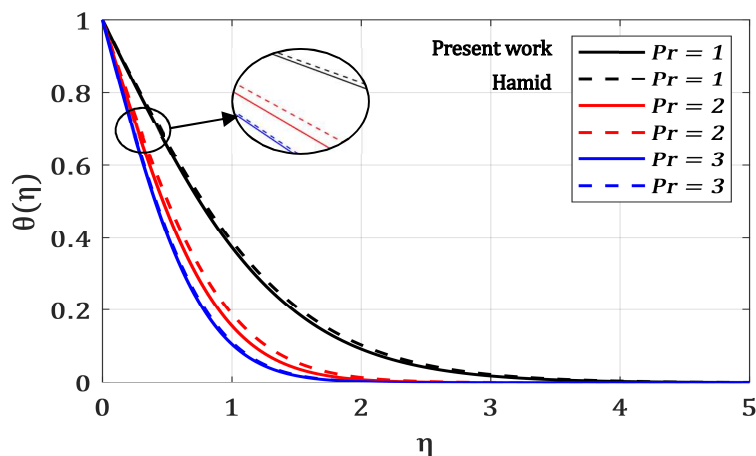


Fig. 8. Effect of Prandtl number on the temperature distribution when  $\gamma = 0.02, \gamma_\varphi = 2$  (solid for the present work) and (dotted for Fig. 16 in Hamid [35])

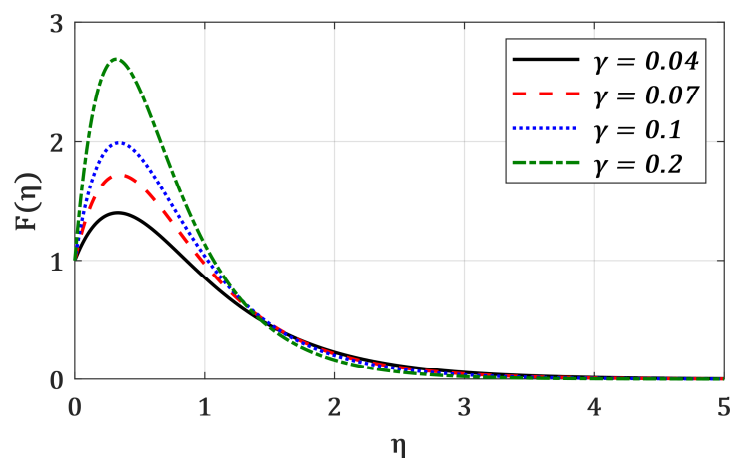


Fig. 9. Effect of ratio of temperature difference on nanofluid velocity inside the boundary layer when  $Pr = 4, \gamma_\varphi = 2$  ( $Al_2O_3$ -water)

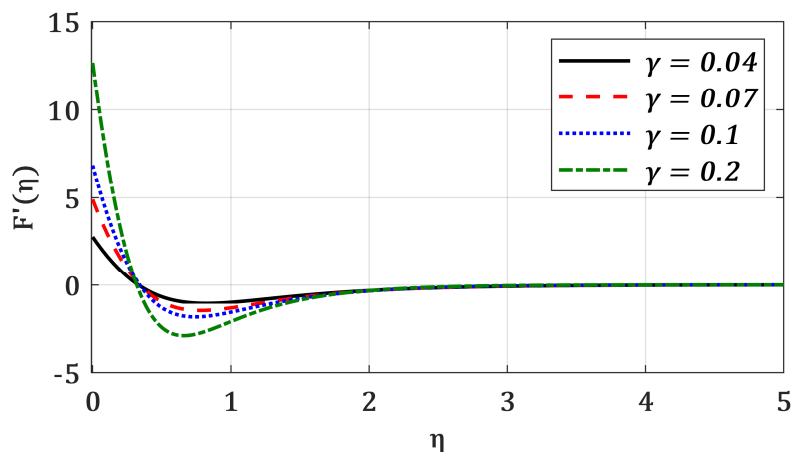
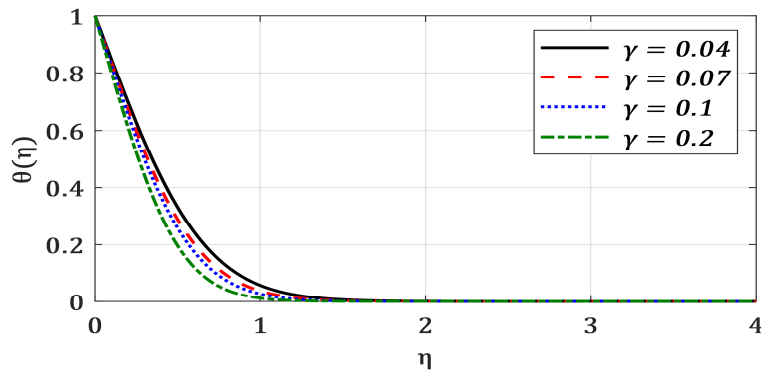


Fig. 10. Effect of ratio of temperature difference on nanofluid shear stress inside the boundary layer when  $Pr = 4, \gamma_\varphi = 2$  ( $Al_2O_3$ -water)

#### 4.2 Effect of ratio of temperature difference, $\gamma$

The ratio of temperature difference is evaluated as  $(\gamma = (T_w - T_\infty) / T_\infty)$  with the following range  $(0.04 \leq \gamma \leq 0.2)$ . The recent study is motivated also by analyzing the effect of heating the plate such that a temperature difference,  $\Delta T = T_w - T_\infty$  arises resulting in an increase in  $\gamma$  values. Figure 9 illustrates an obvious increase in fluid velocity inside the boundary layer due to the increase in  $\gamma$  values. It is observed that the fluid velocity increases far away from the plate surface to peak value and reduces to zero satisfying the boundary conditions. This may be due to the higher kinetic energy gained by the nanofluid particles as a result of the thermal energy. A relevant increase in shear stress has been noticed and illustrated in Fig. 10. On the other hand,  $\gamma$  values have an inverse effect on heat distribution which is depicted in Fig. 11. As a result, the heat flux is increased as  $\gamma$  values increase as shown in Fig. 12.





**Fig. 11.** Effect of ratio of temperature difference on temperature distribution inside the boundary layer when  $Pr = 4, \gamma_\varphi = 2$  ( $\text{Al}_2\text{O}_3$ -water)

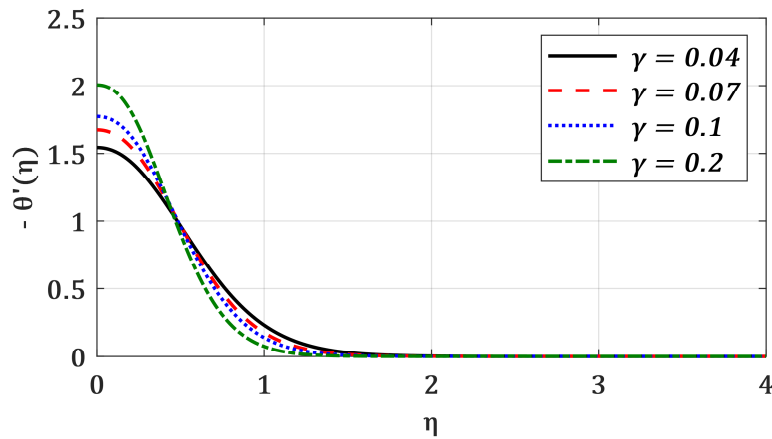


**Fig. 12.** Effect of ratio of temperature difference on heat flux inside the boundary layer when  $Pr = 4, \gamma_\varphi = 2$  ( $\text{Al}_2\text{O}_3$ -water)

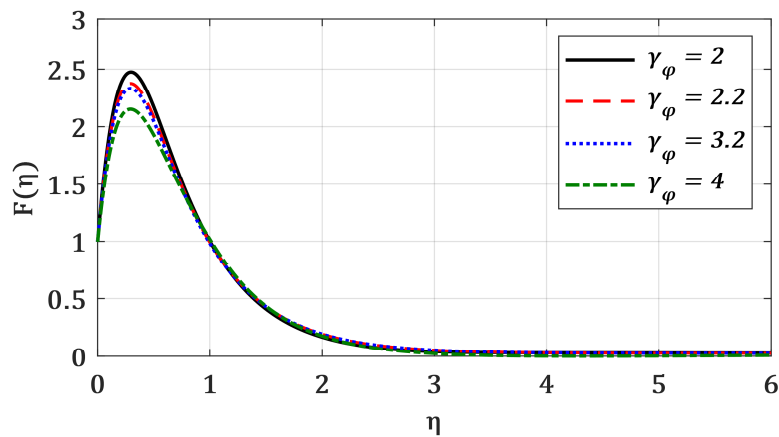


**Fig. 13.** Effect of ratio of nanoparticles volumetric fraction difference on nanofluid velocity inside the boundary layer when  $Pr = 6, \gamma = 0.05$  ( $\text{Al}_2\text{O}_3$ -water)

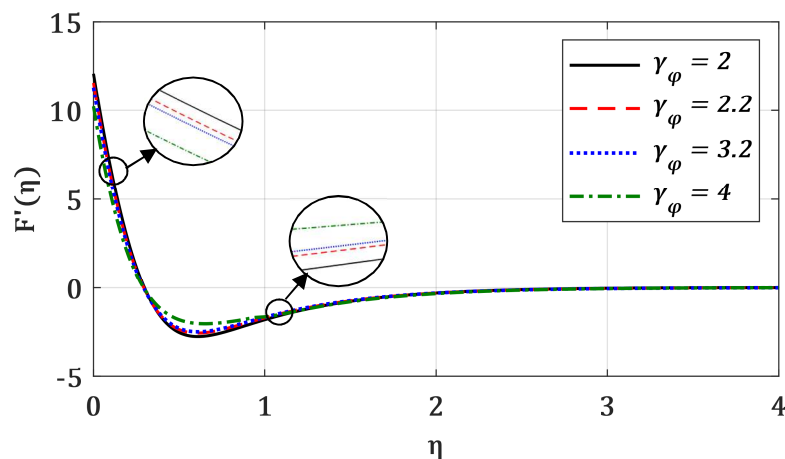


**Fig. 14.** Effect of ratio of nanoparticles volumetric fraction difference on shear stress inside the boundary layer when  $Pr = 6, \gamma = 0.05$  ( $\text{Al}_2\text{O}_3$ -water)



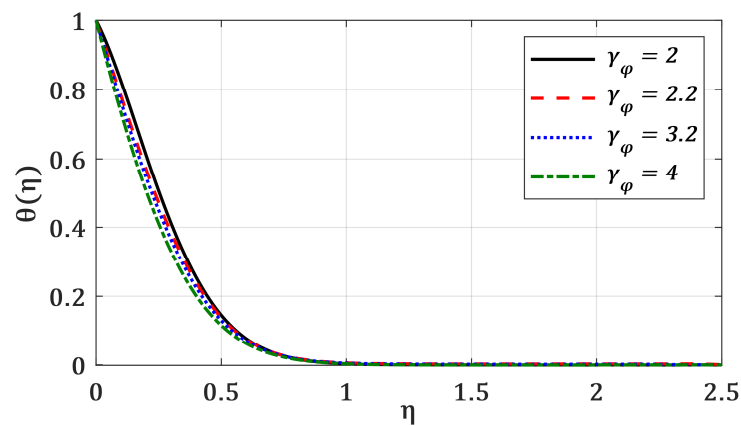


**Fig. 15.** Effect of ratio of nanoparticles volumetric fraction difference on temperature distribution inside the boundary layer when  $Pr = 6, \gamma = 0.05$  ( $Al_2O_3$ -water)

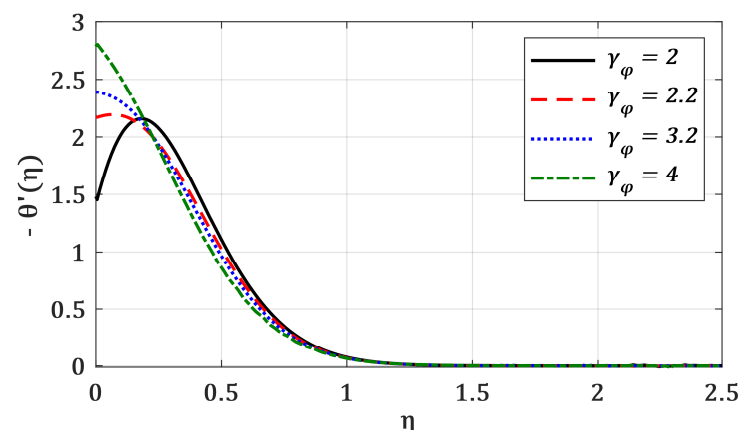


**Fig. 16.** Effect of ratio of nanoparticles volumetric fraction difference on heat flux inside the boundary layer when  $Pr = 6, \gamma = 0.05$  ( $Al_2O_3$ -water)

#### 4.3 Effect of ratio of nanoparticles volumetric fraction difference, $\gamma_\phi$

The ratio of nanoparticles volumetric fraction difference is evaluated as  $\gamma_\phi$  with range ( $2 \leq \gamma_\phi \leq 4$ ). The effects of volumetric fraction of nanoparticles on velocity and related shear stress are illustrated in Figs.13 and 14. It is noticed that velocity profile is decreased by increasing the volume fraction of nanoparticles as seen in Fig. 13. A relevant decrease in shear stress has been noticed and illustrated in Fig.14. Increasing  $\gamma_\phi$  leads to a decrease in velocity profile due to the increase in the resistance between the adjacent moving layers of the fluid. On the other hand, Fig. 15 shows a decrease in temperature distribution inside the boundary layer accompanied by a relevant increase in heat flux as shown in Fig. 16 due to the high thermal diffusivity gained by the nanoparticles.

According to the form of Nusselt number as shown in (46), the Nusselt number ( $Nu$ ) is described as a measure of a dimensionless temperature gradient. The numerical values of Nusselt number for different type of nanofluid are presented in Tables 3, 4 and 5.

**Table 3.** Effects of the Prandtl number ( $Pr$ ) for different types of nanofluids on Nusselt number when  $\gamma = 0.05, \gamma_\phi = 2$

Pr	Nanoparticles			
	Cu	$Al_2O_3$	Ag	$TiO_2$
2	1.147461	1.21751417	1.271504	1.3086276
3	1.3613125	1.43649509	1.494979	1.5354041
4	1.5386024	1.61672195	1.677978	1.7205123
5	1.693500	1.77338089	1.836463	1.8804425

**Table 4.** Effects of the ratio of temperature difference  $\gamma$  for different types of nanofluids on Nusselt number when  $Pr = 4, \gamma_\phi = 2$

$\gamma$	Nanoparticles			
	Cu	$Al_2O_3$	Ag	$TiO_2$
0.04	1.623808	1.544023	1.669437	1.697519
0.07	1.755129	1.673476	1.801689	1.830259
0.1	1.855905	1.772328	1.903465	1.932579
0.2	2.093980	2.004843	2.144506	2.175231

**Table 5.** Effects of the ratio of nanoparticles volumetric fraction  $\gamma_\phi$  for different types of nanofluids on Nusselt number when  $Pr = 6, \gamma = 0.05$

$\gamma_\phi$	Nanoparticles			
	Cu	$Al_2O_3$	Ag	$TiO_2$
2	2.32450	1.516050	2.323778	2.297028
2.2	2.403130	2.182780	2.40005	2.367670
3.2	2.436577	2.381617	2.435811	2.399810
4	2.470093	2.759079	2.469310	2.430141



**Table 6.** Effects of the Prandtl number (Pr) for different types of nanofluids on Sherwood number when  $Pr = 6, \gamma = 0.05$ 

Pr	Nanoparticles		
	Cu	Al <sub>2</sub> O <sub>3</sub>	TiO <sub>2</sub>
2	0.10181824	0.0879777	0.099002
3	0.1361666	0.220304	0.1326768
4	0.1697519	0.377440	0.165704
5	0.2017548	0.540040	0.197222

The tables indicate that the values of Nusselt number depends on the types of nanoparticles. This leads to change the rate of heat transfer. Therefore, the types of nanofluid are important in the cooling and heating processes. From tables 3 and 4, it is observed that (TiO<sub>2</sub>-water) nanofluid has higher Nusselt number compared to other nanofluids. Also, it can be seen from table 5 that the (Cu-water) nanofluid achieves higher values of Nusselt number. Table 6 displays the variation of the Sherwood number with different types of nanofluid. Table 6 shows that Sherwood number increases as Prandtl number increases.

## 5. Conclusion

Nanofluid characteristics have been investigated throughout nonhomogeneous nanoparticles distribution inside the boundary layer adjacent to a vertical moving plate. The recent study assumes a temperature dependence of Brownian diffusion coefficient and a nanoparticles fraction dependence of thermal diffusion coefficient inside the boundary layer. The study is motivated by analyzing the effect of Prandtl number, the ratio of temperature difference and the ratio of nanoparticle volumetric fractions on the nanofluid velocity, shear stress, temperature distribution, heat flux, nanoparticles distribution and nanoparticle gradient inside the boundary layer. The results show that the nanofluid velocity has a decremental relation with increasing both Pr and  $\gamma_\phi$  values whereas it has an incremental relation with  $\gamma$  values. The shear stress in nanofluid layers is proportionally related to  $\gamma$  values but inversely related to Pr and  $\gamma_\phi$  values. Moreover, the temperature distribution inside the boundary layer is affected inversely by all parameters, Pr,  $\gamma$  and  $\gamma_\phi$  values. On the other hand, the heat flux throughout the boundary layer is affected proportionally. The volumetric nanoparticles fraction and its gradient distributions are decreased and increased, respectively with the increase of Pr values. It was found that (TiO<sub>2</sub>-water) nanofluid that has lower thermal conductivity has better Nusselt number compared to other nanofluids. Increase in values of Prandtl number tends to increase the Sherwood number.

## Author Contributions

A.S. Rashed: Conceptualization, methodology, analysis, review and editing. Tarek A. Mahmoud: Methodology, programming, analysis and writing. M.M. Kassem: Review and editing.

## Conflict of Interest

The authors declared no potential conflicts of interest with respect to the research, authorship, and publication of this article.

## Funding

The authors received no financial support for the research, authorship, and publication of this article.

## Nomenclature

### Latin symbols

$a$	Group parameter
$C_{bf}$	Specific heat of the base fluid [J/Kg K]
$C_{np}$	Specific heat of the nanoparticle [J/Kg K]
$D_B$	Brownian diffusion coefficient [m <sup>2</sup> /sec]
$D_T$	Thermal diffusion coefficient [m <sup>2</sup> /sec]
$d_p$	Nanoparticle diameter [m]
$F$	Dimensionless velocity
$G$	Group symbol
$g$	Acceleration of gravity [9.81 m/sec <sup>2</sup> ]
$K_B$	Boltzmann constant [ $1.380649 \times 10^{-23}$ J/K]
$K_{bf}$	Base fluid thermal conductivity [W/m K]
$Nu$	Nusselt number
$Pr$	Prandtl number
$Q$	Real-valued coefficient
$Sh$	Sherwood number
$T$	Temperature [K]
$T_w$	Wall temperature of the vertical plate [K]
$T_\infty$	Ambient temperature [K]
$(u, v)$	Velocity components
$u_w$	Wall velocity
$(x, y)$	Cartesian coordinates

### Greek symbols

$\alpha$	Thermal diffusivity [m <sup>2</sup> /sec]
$\gamma$	Ratio of temperature differences to ambient temperature ( $T_w - T_\infty$ ) / $T_\infty$
$\gamma_\infty$	Ratio of nanoparticles volumetric fraction difference to ambient fraction ( $\phi_w - \phi_\infty$ ) / $\phi_\infty$
$\eta$	Similarity variable
$\theta$	Dimensionless temperature
$\mu$	Dynamic viscosity [Pa s]
$\nu$	Kinematic viscosity [m <sup>2</sup> /sec]
$\rho_{bf}$	Density of base fluid [Kg/m <sup>3</sup> ]
$\rho_{np}$	Density of the nanoparticle [Kg/m <sup>3</sup> ]
$\phi$	Nanoparticle volumetric fraction
$\phi_w$	Nanoparticle volume fraction at the wall
$\phi_\infty$	Ambient nanoparticle volume fraction

### Subscript

bf	Base fluid
np	Nanoparticle
w	Condition on the wall
$\infty$	Condition far away from the surface

### Superscript

'	Differentiation with respect to $\eta$
---	--



## References


- [1] Khanafer, K., Vafai, K., and Lightstone, M. Buoyancy-driven heat transfer enhancement in a two-dimensional enclosure utilizing nanofluids. *International Journal of Heat and Mass Transfer*, 46(19), 2003, 3639-3653.
- [2] Abu-Nada, E., Masoud, Z., and Hijazi, A. Natural convection heat transfer enhancement in horizontal concentric annuli using nanofluids. *International Communications in Heat and Mass Transfer*, 35(5), 2008, 657-665.
- [3] Haghshenas Fard, M., Esfahany, M.N., and Talaie, M.R. Numerical study of convective heat transfer of nanofluids in a circular tube two-phase model versus single-phase model. *International Communications in Heat and Mass Transfer*, 37(1), 2010, 91-97.
- [4] Lotfi, R., Rashidi, A.M., and Saboohi, Y. Numerical study of forced convective heat transfer of Nanofluids: Comparison of different approaches. *International Communications in Heat and Mass Transfer*, 37(1), 2010, 74-78.
- [5] Sheikholeslami, M. and Ganji, D.D. Nanofluid convective heat transfer using semi analytical and numerical approaches: A review. *JTICE Journal of the Taiwan Institute of Chemical Engineers*, 65, 2016, 43-77.
- [6] Sheikholeslami, M. and Ganji, D.D. Nanofluid hydrothermal behavior in existence of Lorentz forces considering Joule heating effect. *Journal of Molecular Liquids*, 224, 2016, 526-537.
- [7] Buongiorno, J. Convective Transport in Nanofluids. *Journal of Heat Transfer*, 128(3), 2005, 240-250.
- [8] Xu, H., Wang, Z., Wu, J., Li, Q., Liu, M., and Li, Y. Mechanical properties and microstructure of Ti/Al<sub>2</sub>O<sub>3</sub> composites with Pr<sub>6</sub>O<sub>11</sub> addition by hot pressing sintering. *Materials & Design*, 101, 2016, 1-6.
- [9] Hirvikorpi, T., Vähä-Nissi, M., Nikkila, J., Harlin, A., and Karppinen, M. Thin Al<sub>2</sub>O<sub>3</sub> barrier coatings onto temperature-sensitive packaging materials by atomic layer deposition. *Surface and Coatings Technology*, 205(21), 2011, 5088-5092.
- [10] Dehm, G., Scheu, C., Rühle, M., and Raj, R. Growth and structure of internal Cu/Al<sub>2</sub>O<sub>3</sub> and Cu/Ti/Al<sub>2</sub>O<sub>3</sub> interfaces. Paper presented at Sympos. Synergistic Synthesis of Inorganic Materials. *Acta Materialia*, 46(3), 1998, 759-772.
- [11] Lukic, I., Krstic, J., Jovanovic, D., and Skala, D. Alumina/silica supported K<sub>2</sub>CO<sub>3</sub> as a catalyst for biodiesel synthesis from sunflower oil. *BITE Bioresource Technology*, 100(20), 2009, 4690-4696.
- [12] Khan, W.A. and Aziz, A. Natural convection flow of a nanofluid over a vertical plate with uniform surface heat flux. *International Journal of Thermal Sciences*, 50(7), 2001, 1207-1214.
- [13] Thompson, L. and Argonne National Laboratory, A.I.L. Anomalous increased effective thermal conductivities of ethylene glycol-based nanofluids containing copper nanoparticles. *Applied Physics Letters*, 78(6), 2001, 718-720.
- [14] Aziz, A. and Khan, W.A. Natural convective boundary layer flow of a nanofluid past a convectively heated vertical plate. *International Journal of Thermal Sciences*, 52, 2012, 83-90.
- [15] Rahman, M.M. and Eltayeb, I.A. Radiative heat transfer in a hydromagnetic nanofluid past a non-linear stretching surface with convective boundary condition. *Meccanica*, 48(3), 2013, 601-615.
- [16] Siddiqua, S., Begum, N., Hossain, M.A., Gorla, R.S.R., and Al-Rashed, A.A. Two-phase natural convection dusty nanofluid flow. *International Journal of Heat and Mass Transfer*, 118, 2018, 66-74.
- [17] Ibrahim, S.M. and Bhashar Reddy, N. Similarity Solution of Heat and Mass Transfer for Natural Convection over a Moving Vertical Plate with Internal Heat Generation and a Convective Boundary Condition in the Presence of Thermal Radiation, Viscous Dissipation, and Chemical Reaction. *ISRN Thermodynamics*, 2013, 2013, 1-10.
- [18] Aly, E. Radiation and MHD Boundary Layer Stagnation-Point of Nanofluid Flow towards a Stretching Sheet Embedded in a Porous Medium: Analysis of Suction/Injection and Heat Generation/Absorption with Effect of the Slip Model. *Mathematical Problems in Engineering*, 2015, 2015, 1-20.
- [19] Elgazery, N.S. Nanofluids flow over a permeable unsteady stretching surface with non-uniform heat source/sink in the presence of inclined magnetic field. *Journal of the Egyptian Mathematical Society*, 27(1), 2019, 1-26.
- [20] Maskeen, M.M., Zeeshan, A., Mehmood, O.U., and Hassan, M. Heat transfer enhancement in hydromagnetic aluminacopper/water hybrid nanofluid flow over a stretching cylinder. *Journal of Thermal Analysis and Calorimetry*, 138(2), 2019, 1127-1136.
- [21] Ferdows, M., Islam, S., and Quadir, R.A. Similarity solutions of Marangoni heat transfer flow of water based nanofluid containing nanoparticles with variable viscosity and thermal conductivity. *International Review of Mechanical Engineering*, 7(4), 2013, 692-697.
- [22] Aly, E.H. Radiation and MHD Boundary Layer Stagnation-Point of Nanofluid Flow towards a Stretching Sheet Embedded in a Porous Medium: Analysis of Suction/Injection and Heat Generation/Absorption with Effect of the Slip Model. *Mathematical Problems in Engineering*, 2015, 2015, 563547.
- [23] Yacob, N.A., Ishak, A., Nazar, R., and Pop, I. Mixed Convection Flow Adjacent to a Stretching Vertical Sheet in a Nanofluid. *Journal of Applied Mathematics*, 2013, 2013, 696191.
- [24] Bagheri, A., Gholami, H., and Maghsoudi, M. Natural convective boundary-layer flow of a nanofluid past a vertical plate with heat flux condition. *International Research Journal of Applied & Basic Sciences*, 5, 2013, 1406-1414.
- [25] Sheikholeslami, M. New computational approach for exergy and entropy analysis of nanofluid under the impact of Lorentz force through a porous media. *Computer Methods in Applied Mechanics and Engineering*, 344, 2018, 319-333.
- [26] Sheikholeslami, M. Numerical simulation for solidification in a LHTSS by means of nano-enhanced PCM. *Journal of the Taiwan Institute of Chemical Engineers*, 86, 2018, 25-41.
- [27] Khan, I., Shah, N.A., and Dennis, L.C.C. A scientific report on heat transfer analysis in mixed convection flow of Maxwell fluid over an oscillating vertical plate. *Scientific Reports*, 7(1), 2017, 40147.
- [28] Khan, A., Khan, D., Khan, I., Ali, F., Karim, F., and Imran, M. MHD Flow of Sodium Alginate-Based Casson Type Nanofluid Passing Through A Porous Medium With Newtonian Heating. *Scientific Reports*, 8(1), 2018, 8645.
- [29] Anwar, T., Kumam, P., and Watthayu, W. An exact analysis of unsteady MHD free convection flow of some nanofluids with ramped wall velocity and ramped wall temperature accounting heat radiation and injection/consumption. *Scientific Reports*, 10(1), 2020, 17830.
- [30] Sui, J., Zhao, P., Bin-Mohsin, B., Zheng, L., Zhang, X., Cheng, Z., Chen, Y., and Chen, G. Fractal aggregation kinetics contributions to thermal conductivity of nano-suspensions in unsteady thermal convection. *Scientific Reports*, 6(1), 2016, 39446.
- [31] Khan, N.S., Shah, Q., Bhaumik, A., Kumam, P., Thounthong, P., and Amiri, I. Entropy generation in bioconvection nanofluid flow between two stretchable rotating disks. *Scientific Reports*, 10(1), 2020, 4448.
- [32] Ali, F., Aamina, Khan, I., Sheikh, N.A., Gohar, M., and Tlili, I. Effects of Different Shaped Nanoparticles on the Performance of Engine-Oil and Kerosene-Oil: A generalized Brinkman-Type Fluid model with Non-Singular Kernel. *Scientific Reports*, 8(1), 2018, 15285.
- [33] El-Zahar, E.R., Rashad, A.M., Saad, W., and Seddek, L.F. Magneto-Hybrid Nanofluids Flow via Mixed Convection past a Radiative Circular Cylinder. *Scientific Reports*, 10(1), 2020, 10494.
- [34] Sobamowo, M.G., Yinusa, A., and Makinde, O.D. A Study on the Effects of Inclined Magnetic Field, Flow Medium Porosity and Thermal Radiation on Free Convection of Casson Nanofluid over a Vertical Plate. *World Scientific News*, 138(1), 2019, 1-64.
- [35] Hamid, A., Hashim, Khan, M., and Alghamdi, M. MHD Blasius flow of radiative Williamson nanofluid over a vertical plate. *International Journal of Modern Physics B*, 33(22), 2019, 1950245.
- [36] Nallagundla, N., Amanulla, C., Reddy, M., and Prasad, V.R. Hydromagnetic Flow of Heat and Mass Transfer in a Nano Williamson Fluid Past a Vertical Plate With Thermal and Momentum Slip Effects: Numerical Study. *Nonlinear Engineering*, 8, 2018.
- [37] Narahari, M., Suresh Kumar Raju, S., and Pendyala, R. Unsteady natural convection flow of multi-phase nanofluid past a vertical plate with constant heat flux. *Chemical Engineering Science*, 167, 2017, 229-241.
- [38] Natural convective magneto-nanofluid flow and radiative heat transfer past a moving vertical plate. *Alexandria Engineering Journal*, 54(1), 2015, 55-64.
- [39] Rahmana, M. and Aziz, A. Heat transfer in water based nanofluids (TiO<sub>2</sub>-H<sub>2</sub>O, Al<sub>2</sub>O<sub>3</sub>-H<sub>2</sub>O and Cu-H<sub>2</sub>O) over a stretching cylinder. *International Journal of Heat and Technology*, 30(02), 2012, 31-42.
- [40] Sheikholeslami, M. and Ganji, D.D. Numerical investigation for two phase modeling of nanofluid in a rotating system with permeable sheet. *Journal of Molecular Liquids*, 194, 2014, 13-19.
- [41] Sheikholeslami, M. and Ganji, D.D. Heat transfer of Cu-water nanofluid flow between parallel plates. *Powder Technology*, 235, 2013, 873-879.
- [42] Tibaut, J., Tibaut, T., and Ravník, J. Numerical simulation of mixed convection of a nanofluid in a circular pipe with different numerical models.





*Journal of Thermal Analysis and Calorimetry*, 2020, DOI: 10.1007/s10973-020-09727-3.

- [43] Jayachandra Babu, M., Sandeep, N., and Saleem, S. Free convective MHD Cattaneo-Christov flow over three different geometries with thermophoresis and Brownian motion. *Alexandria Engineering Journal*, 56(4), 2017, 659-669.
- [44] Mabrouk, S.M. and Rashed, A.S. Analysis of  $(3 + 1)$ -dimensional Boiti – Leon –Manna–Pempinelli equation via Lax pair investigation and group transformation method. *Computers & Mathematics with Applications*, 74(10), 2017, 2546-2556.
- [45] Rashed, A.S. Analysis of  $(3+1)$ -dimensional unsteady gas flow using optimal system of Lie symmetries. *Mathematics and Computers in Simulation*, 156, 2019, 327-346.
- [46] Rashed, A.S. and Kassem, M.M. Group analysis for natural convection from a vertical plate. *Journal of Computational and Applied Mathematics*, 222(2), 2008, 392-403.
- [47] Kassem, M.M. and Rashed, A.S. Group solution of a time dependent chemical convective process. *Applied Mathematics and Computation*, 215(5), 2009, 1671-1684.
- [48] Rashed, A.S. and Kassem, M.M. Hidden symmetries and exact solutions of integro-differential Jaulent-Miodek evolution equation. *Applied Mathematics and Computation*, 247, 2014, 1141-1155.
- [49] Kassem, M.M. and Rashed, A.S. N-solitons and cuspon waves solutions of  $(2 + 1)$ -dimensional Broer–Kaup–Kupershmidt equations via hidden symmetries of Lie optimal system. *Chinese Journal of Physics*, 57, 2019, 90-104.
- [50] Mabrouk, S.M. and Rashed, A.S. N-Solitons, kink and periodic wave solutions for  $(3 + 1)$ -dimensional Hirota bilinear equation using three distinct techniques. *Chinese Journal of Physics*, 60, 2019, 48-60.
- [51] Saleh, R. and Rashed, A.S. New exact solutions of  $(3 + 1)$ dimensional generalized Kadomtsev Petviashvili equation using a combination of lie symmetry and singular manifold methods. *Mathematical Methods in the Applied Sciences*, 43(4), 2020, 2045-2055.
- [52] Moran, M.J., Gaggioli, R.A., and Scholten, W.B., A new systematic formalism for similarity analysis, with applications to boundary layer flows. Madison, Wis.: Mathematics Research Center, United States Army, University of Wisconsin, 1968.
- [53] Abd-El-Malek, M.B., Boutros, Y.Z., and Badran, N.A. Group method analysis of unsteady free-convective laminar boundary-layer flow on a nonisothermal vertical flat plate. *Journal of Engineering Mathematics*, 24(4), 1990, 343-368.
- [54] Abd-el-Malek, M.B., Kassem, M.M., and Mekky, M.L. Similarity solutions for unsteady free-convection flow from a continuous moving vertical surface. *Journal of Computational and Applied Mathematics*, 164-165, 2004, 11-24.
- [55] Buongiorno, J. Convective Transport in Nanofluids. *Journal of Heat Transfer*, 128(3), 2006, 240-250.
- [56] Sobamowo, G. Free Convection Flow and Heat Transfer of Nanofluids of Different Shapes of Nano-Sized Particles over a Vertical Plate at Low and High Prandtl Numbers. *Journal of Applied and Computational Mechanics*, 5, 2019, 13-39.
- [57] Bird, R.B., Stewart, W.E., and Lightfoot, E.N., Transport phenomena. New York: University of Wisconsin, 1960.
- [58] Abu-Nada, E. and Oztop, H.F. Effects of inclination angle on natural convection in enclosures filled with Cu-water nanofluid. *International Journal of Heat and Fluid Flow*, 30(4), 2009, 669-678.
- [59] Mohd Zin, N.A., Khan, I., Shafie, S., and Alshomrani, A.S. Analysis of heat transfer for unsteady MHD free convection flow of rotating Jeffrey nanofluid saturated in a porous medium. *Results in Physics*, 7, 2017, 288-309.
- [60] Morgan, A.J.A. The reduction by one of the number of independent variables in some systems of partial differential equations. *The Quarterly Journal of Mathematics*, 3(1), 1952, 250-259.
- [61] SINGH, K.D. and KUMAR, R. Fluctuating Heat and Mass Transfer on Unsteady MHD Free Convection Flow of Radiating and Reacting Fluid Past a Vertical Porous Plate in Slip- Flow Regime. *Journal of Applied Fluid Mechanics*, 4(4), 2011, 101-106.

## ORCID iD

A.S. Rashed  <https://orcid.org/0000-0001-7800-2768>

Tarek A. Mahmoud  <https://orcid.org/0000-0001-8846-0877>

M. M. Kassem  <https://orcid.org/0000-0003-3068-6923>



© 2021 Shahid Chamran University of Ahvaz, Ahvaz, Iran. This article is an open access article distributed under the terms and conditions of the Creative Commons Attribution-NonCommercial 4.0 International (CC BY-NC 4.0 license) (<http://creativecommons.org/licenses/by-nc/4.0/>).

How to cite this article: Rashed A.S., Mahmoud T.A., Kassem M.M. Behavior of Nanofluid with Variable Brownian and Thermal Diffusion Coefficients Adjacent to a Moving Vertical Plate, *J. Appl. Comput. Mech.*, 7(3), 2021, 1466–1479.  
<https://doi.org/10.22055/JACM.2021.34852.2483>

**Publisher's Note** Shahid Chamran University of Ahvaz remains neutral with regard to jurisdictional claims in published maps and institutional affiliations.

